

# Binding of hydrogen on benzene, coronene, and graphene from quantum Monte Carlo calculations

Jie Ma,<sup>1,2,3</sup> Angelos Michaelides,<sup>2,3,4</sup> and Dario Alfè<sup>3,4,5,6,a)</sup>

<sup>1</sup>*Institute of Physics, Chinese Academy of Sciences, P.O. Box 603, Beijing 100190, China*

<sup>2</sup>*Department of Chemistry, University College London, Gower Street, London WC1E 6BT, United Kingdom*

<sup>3</sup>*London Centre for Nanotechnology, University College London, 17-19 Gordon Street, London WC1H 0AH, United Kingdom*

<sup>4</sup>*Thomas Young Centre@UCL, University College London, Gower Street, London WC1E 6 BT, United Kingdom*

<sup>5</sup>*Department of Earth Sciences, University College London, Gower Street, London WC1E 6BT, United Kingdom*

<sup>6</sup>*Department of Physics and Astronomy, University College London, Gower Street, London WC1E 6BT, United Kingdom*

(Received 21 January 2011; accepted 1 March 2011; published online 4 April 2011)

Quantum Monte Carlo calculations with the diffusion Monte Carlo (DMC) method have been used to compute the binding energy curves of hydrogen on benzene, coronene, and graphene. The DMC results on benzene agree with both Møller–Plessett second order perturbation theory (MP2) and coupled cluster with singles, doubles, and perturbative triples [CCSD(T)] calculations, giving an adsorption energy of  $\sim 25$  meV. For coronene, DMC agrees well with MP2, giving an adsorption energy of  $\sim 40$  meV. For physisorbed hydrogen on graphene, DMC predicts a very small adsorption energy of only  $5 \pm 5$  meV. Density functional theory (DFT) calculations with various exchange-correlation functionals, including van der Waals corrected functionals, predict a wide range of binding energies on all three systems. The present DMC results are a step toward filling the gap in accurate benchmark data on weakly bound systems. These results can help us to understand the performance of current DFT based methods, and may aid in the development of improved approaches.

© 2011 American Institute of Physics. [doi:10.1063/1.3569134]

## I. INTRODUCTION

Hydrogen is the most abundant element in the Universe. It is the fuel of stars and the originator of all other elements. In the interstellar medium (ISM), hydrogen is mostly present as single isolated atoms. However, there is also evidence of relatively large abundances of molecular hydrogen (in fact, H<sub>2</sub> is the most abundant molecule in the Universe), despite the continued dissociation caused by stellar ultraviolet radiation and cosmic rays. The rate of formation of molecular hydrogen is much larger than what could be achieved in the gas phase, if one takes into account the low density of atomic hydrogen in space and the absence of an efficient mechanism to dissipate the kinetic energy of the collisions. Therefore, it is generally believed that molecular hydrogen forms on the surface of dust grains that act as catalytic sites for the recombination of atomic hydrogen. These dust grains come in different shapes, sizes, and compositions. The largest ones are thought to be formed by silicate cores covered by organic mantles and icy surfaces, while the smallest ones may be entirely carbonaceous or even simple polycyclic aromatic hydrocarbons (PAHs). It is thus possible that molecular hydrogen formation may occur on PAHs (Refs. 1 and 2) or even simply on graphitic surfaces, which would act as aggregation sites, locally increasing hydrogen concentration and therefore facilitating atomic encounters (Ref. 3 and references

therein). The interaction of hydrogen with graphitic surfaces has also sparked significant interest recently, thanks to the possible role of these surfaces as hydrogen storage media for mobile applications (see, e.g., Ref. 4). At much higher energies the interaction between hydrogen and graphite is important to understand in controlled fusion devices called tokamaks, which magnetically confine high energy plasmas but cannot avoid high energy particle bombardment of their graphitic internal walls. These and other arguments justify the interest in understanding the interaction of hydrogen with carbonaceous materials, and in particular its binding on their surfaces.

Atomic hydrogen on graphite chemisorbs on top a carbon atom with a binding energy in the region of 0.6–0.7 eV (60–70 kJ/mole).<sup>5,6</sup> The carbon atom involved in the bonding is pulled out from the graphitic plane by about 0.4 Å, giving rise to an activation energy of about 0.2 eV (Ref. 7) to get to the chemisorbed state. These relatively large numbers suggest that graphite (or, which is the same for present purposes, graphene, which is a single layer of graphite) catalyzed molecular hydrogen formation at ISM temperatures is highly unlikely from the chemisorbed hydrogen state. It has therefore been postulated that there must exist a physisorbed minimum, with a much lower binding energy, allowing the physisorbed atoms to diffuse relatively rapidly. Such a physisorbed state indeed appears to have been observed experimentally, although the experimental evidence is neither abundant nor recent.<sup>8</sup>

<sup>a)</sup>Electronic mail: d.alfè@ucl.ac.uk.

For the above reasons, effort has been devoted to try to calculate the adsorption energy of this possible physisorbed state; however, this is less straightforward than it may appear at first sight. The reason is that the forces holding H to a graphitic layer are weak and of dispersive nature, so standard quantum mechanics methods based on density functional theory (DFT) have difficulties in achieving satisfactory accuracy to describe these forces, although recent developments in this area are slowly changing this.<sup>9–11</sup> On the other hand, high accuracy quantum chemistry methods are expensive and difficult to apply in large systems. Recently, Bofanti *et al.*<sup>3</sup> tried to address this problem by finding a compromise between accuracy and size in calculating the binding energy curve of H on benzene and coronene (an aromatic molecule formed by seven connected carbon hexagons terminated with hydrogens) using Møller–Plesset second order perturbation theory (MP2). For dispersion bonded systems, MP2 often outperforms DFT with standard exchange–correlation functionals, but is not as accurate as full configuration interaction or coupled cluster techniques [e.g., coupled cluster with singles, doubles, and perturbative triples (CCSD(T))], although for H on benzene MP2 and CCSD(T) agree almost perfectly.<sup>3</sup> Hydrogen on coronene was deemed to be a good model for a H–graphene system, and led the authors to report a binding energy for the physisorbed state in the region of 40 meV. Indeed, this value agrees quite closely with the experimental value of Ghio *et al.*<sup>8</sup> However, the argument that coronene, a molecule with a large HOMO–LUMO gap, is a good model for graphene, which is a semimetal, is weak and has not been proven. Moreover, the accuracy of MP2 may not be sufficient to provide a reliable H–coronene binding energy, and the accuracy of MP2 diminishes as the cluster increases in size and the band gap of the system is reduced. Thus, with traditional quantum chemistry or DFT it is difficult, if not impossible, to obtain accurate physisorption energies for those systems, which presents a great opportunity for the application of quantum Monte Carlo (QMC).

Here, we have used QMC techniques to compute the binding energy of (i) hydrogen on benzene, (ii) hydrogen on coronene, and (iii) that of hydrogen on graphene. Specifically, we have applied diffusion Monte Carlo within the fixed node (DMC-FN) pseudopotential scheme.<sup>12</sup> This alternative first principles method, while computationally much more expensive than DFT, is emerging as a robust and accurate *ab initio* approach for treating weakly interacting systems, particularly those in condensed phases (see, for example, Refs. 13 and 14). Being a Monte Carlo method, QMC can also efficiently exploit the power of massively parallel computers, and we have used up to almost 20 000 cores for the present calculations. In our previous work we showed that DMC-FN techniques are indeed extremely accurate for systems involving water, benzene, and graphene,<sup>15,16</sup> and also for systems with zero gap, such as metallic magnesium<sup>17</sup> and iron.<sup>18,19</sup> QMC methods have also been applied to study the interaction of hydrogen with the Si(001) (Ref. 20) and the Mg(0001) (Ref. 21) surfaces.

Here, we find that for hydrogen on benzene QMC agrees very well with both MP2 and CCSD(T) calculations, giving a binding energy of  $\sim 25$  meV. For hydrogen on coronene,

QMC agrees well with MP2, giving an adsorption energy of  $\sim 40$  meV. For the hydrogen on graphene system we find only a very small QMC binding energy of  $5 \pm 5$  meV. We also augmented our calculations by using DFT with various exchange–correlation functionals, which give an unsurprisingly wide range of binding energies. In particular, it is interesting to investigate the performance of recent van der Waals (vdW) corrected functionals, which we find to agree generally better with DMC, but still display some variability.

## II. TECHNIQUES

### A. Quantum Monte Carlo calculations

Diffusion Monte Carlo calculations have been performed with the CASINO code<sup>39</sup> using trial wavefunctions of the Slater–Jastrow type:

$$\Psi_T(\mathbf{R}) = D^\uparrow D^\downarrow e^J, \quad (1)$$

where  $D^\uparrow$  and  $D^\downarrow$  are Slater determinants of up- and down-spin single-electron orbitals, and  $e^J$  is the so-called Jastrow factor, which is the exponential of a sum of one-body (electron–nucleus), two-body (electron–electron), and three-body (electron–electron–nucleus) terms, which are parametrized functions of electron–nucleus, electron–electron, and electron–electron–nucleus separations, and are designed to satisfy the cusp conditions. The parameters in the Jastrow factor are varied to minimize the local energy  $E_L(\mathbf{R}) \equiv \Psi_T^{-1}(\mathbf{R}) \hat{H} \Psi_T(\mathbf{R})$ .<sup>22,23</sup> Imaginary time evolution of the Schrödinger equation has been performed with the usual short time approximation and the locality approximation.<sup>24</sup> For the coronene system we found that DMC simulations with the locality approximation were unstable, and we therefore used the T-move scheme developed by Casula,<sup>25</sup> which treats the nonlocal part of the pseudopotential in a consistent variational scheme and results in a more stable DMC algorithm. We paid careful attention that DMC energy differences were converged with respect to time step errors, particularly for the cases where we used the T-move scheme. We tested time steps of 0.0125 and 0.005 a.u., and found that with a time step of 0.0125 a.u. binding energies were converged to better than 5 meV. With this time step the acceptance ratio was 99.5%.

We used Dirac–Fock pseudopotentials (PP) for C, O, and H.<sup>26</sup> The C and O PPs have a frozen He core and core radii of 0.58 and 0.4 Å, respectively. The H PP has a core radius of 0.26 Å. The single particle orbitals have been obtained by DFT plane wave (PW) calculations using the local density approximation (LDA) and a PW cutoff of 300 Ry (4082 eV), using the PWSCF package,<sup>27</sup> and re-expanded in terms of B-splines,<sup>28</sup> using the natural B-spline grid spacing given by  $a = \pi/G_{\max}$ , where  $G_{\max}$  is the length of the largest vector employed in the PW calculations.

The DMC calculations were performed using the Ewald interaction to model electron–electron interactions. For coronene and benzene we performed the calculations with no periodic boundary conditions, and for graphene we used periodicity only in the two directions parallel to the graphene sheet.

## B. Density functional theory calculations

The DFT calculations have been performed with the plane wave basis set codes CPMD<sup>29</sup> and VASP.<sup>30</sup> For the CPMD calculations we employed Troullier–Martins norm-conserving pseudopotentials<sup>31</sup> with an energy cutoff of 1360 eV. For the VASP calculations we used the projector augmented wave (PAW) method<sup>32,33</sup> with an energy cutoff of 400 eV. We used only  $\Gamma$  point for Brillouin zone sampling. Tests with more  $\mathbf{k}$ -points show negligible difference of adsorption energy. Although the calculation setup of CPMD and VASP are different, the energy curves agree well with each other. We used the LDA, the generalized gradient corrected approximation of Perdew, Burke, and Ernzerhof (PBE),<sup>34</sup> and two different vdW correction methods. The first one is an empirical  $R^{-6}$  correction (DFT-D). In this method, the vdW correction is added to the DFT total energy as

$$E_{\text{vdW}} = \sum_{i,j} \frac{C_{ij}}{R_{ij}^6} f(R_{ij}), \quad (2)$$

where  $C_{ij}$  and  $R_{ij}$  are the vdW coefficients and the distance between atom  $i$  and  $j$ , respectively. The vdW coefficients can be calculated as described by Elstner *et al.*<sup>35</sup>  $f(R_{ij})$  is a damping function which prevents a divergence in the energy as  $R_{ij}$  tends to zero:

$$f(R_{ij}) = \left( 1 - \exp \left[ -3.0 \left( \frac{R_{ij}}{R_{0ij}} \right)^7 \right] \right)^4, \quad (3)$$

where  $R_{0ij}$  is the sum of atomic van der Waals radii. They can be calculated from the vdW radii provided by Gavezzotti and co-workers.<sup>36</sup>

The other method is based on the nonlocal functional proposed by Dion *et al.* (vdW-DF).<sup>9</sup> We have used VASP with our implementation<sup>37</sup> of the vdW-DF correlation using the algorithm of Roman-Perez and Soler.<sup>38</sup> The vdW-DF term is calculated on the sum of the pseudovalence and partial electronic core charge densities, i.e., on the same density that is used to calculate the valence exchange-correlation energy in the PAW method in VASP.

Spin polarized calculations are used throughout, with both DFT and QMC.

Figures 1, 3, and 5 have been made using the XCRYSDEN software.<sup>41</sup>

## III. RESULTS

We now report on the binding energy curves for hydrogen on benzene, coronene, and fully periodic graphene, calculated using DFT with various exchange-correlation functionals, including a number of van der Waals corrected functionals, and with DMC-FN.

### A. Hydrogen on benzene

For the hydrogen on benzene system DMC energies were calculated by placing a hydrogen atom over the center of the benzene ring (see Fig. 1), and varying the perpendicular distance from the plane of the ring between 2.5 and 6 Å. Since we

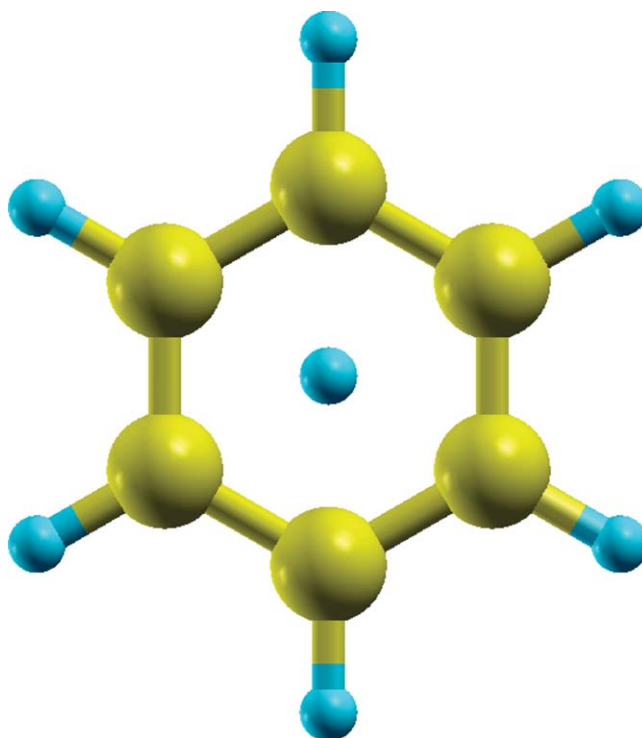


FIG. 1. Top view geometry of the H–benzene system. Carbon atoms are in yellow, hydrogens in blue.

are primarily concerned here with comparing different methods, identical structures are used for all methodologies. The carbon–carbon distance in the benzene ring was 1.397 Å, and the carbon–hydrogen 1.091 Å, which is the PBE geometry.

The DFT calculations were performed by placing the system in a tetragonal box of size  $30 \times 30 \times 36$  a.u.

For the DMC calculations, we used 96 000 walkers distributed on 4800 cores, and simulation lengths of 30 000 steps, resulting in statistical errors of 1.5 meV (one standard deviation). We optimized the Jastrow factor for the system with hydrogen at 3.0 Å from the benzene molecule, and found that we only needed to reoptimize it for the system with the shortest distance of 2.5 Å. The results are displayed in Fig. 2, together with a fit to a Morse potential of the form

$$f(x) = D \{ e^{-2\alpha(x-x_0)} - 2e^{-\alpha(x-x_0)} \}. \quad (4)$$

The parameters of the Morse potentials are reported in Table I.

For the hydrogen on benzene system we can also compare our results with MP2 and CCSD(T) results,<sup>3</sup> which find adsorption energies of 25.3 and 24.8 meV, respectively. The DMC adsorption energy is  $26 \pm 1$  meV, in excellent agreement with the quantum chemistry results. The slightly different geometries in the two sets of calculations are not expected to affect the adsorption energies appreciably.

With DFT, we find that LDA overestimates the interaction considerably when compared with DMC, whereas PBE underestimates it, which is in agreement with previous experience. Correspondingly, LDA and PBE also underestimate and overestimate the equilibrium distance, respectively. The vdW-DF overestimates the adsorption energy by around 10 meV

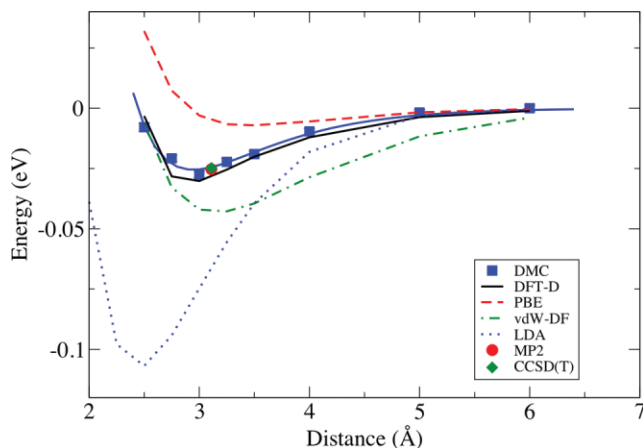


FIG. 2. Binding energy curve for H on benzene. Blue squares and line are DMC calculations and Morse potential fitted to the DMC data, respectively. The DMC error bars are smaller than the size of the points. Red dot: MP2 (Ref. 3); green diamond: CCSD(T) (Ref. 3); black line: DFT-D; red dashed line: PBE; green dashed line: vdW-DF; blue dotted line: LDA.

and also slightly overestimates the equilibrium distance. The DFT-D method agrees well with DMC calculations.

## B. Hydrogen on coronene

For the hydrogen on coronene system, DMC energies were calculated at seven distances between 2.5 and 6.0 Å. The carbon–carbon distances were 1.421 Å, and the carbon–hydrogen 1.07 Å. The geometry of the adsorbed hydrogen was similar to that of the benzene system, with the hydrogen atom over the center of the molecule (see Fig. 3).

The DFT calculations were performed by placing the system in a cubic box of  $36 \times 36 \times 36$  a.u. The structures are

TABLE I. Morse potential parameters [see Eq. (4) in the text] for the DMC physisorption energies of hydrogen on benzene and coronene. MP2 and CCSD(T) data are from Ref. 3. For benzene, the MP2 and CCSD(T) data are single point calculations, with the H atom at a distance of 3.11 Å from the center of the benzene molecule. DFT data with various exchange–correlation functionals are also reported. Error bars are estimated from the Morse fitting procedure.

System	Method	$x_0$ (Å)	D (meV)	$\alpha$ (Å <sup>-1</sup> )
Benzene	DMC	$2.95 \pm 0.03$	$26 \pm 1$	$1.38 \pm 0.09$
	LDA	$2.41 \pm 0.01$	$107 \pm 1$	$1.43 \pm 0.03$
	PBE	$3.44 \pm 0.01$	$7 \pm 0.1$	$1.28 \pm 0.01$
	DFT-D	$2.94 \pm 0.01$	$31 \pm 1$	$1.51 \pm 0.04$
	vdW-DF	$3.14 \pm 0.005$	$43 \pm 0.2$	$1.03 \pm 0.01$
	MP2 (Ref. 3)		25.3	
	CCSD(T) (Ref. 3)		24.8	
Coronene	DMC	$2.94 \pm 0.03$	$43 \pm 2$	$1.47 \pm 0.11$
	LDA	$2.39 \pm 0.01$	$102 \pm 2$	$1.42 \pm 0.04$
	PBE	$3.57 \pm 0.01$	$6 \pm 0.1$	$1.22 \pm 0.01$
	DFT-D	$2.92 \pm 0.01$	$37 \pm 1$	$1.40 \pm 0.05$
	vdW-DF	$2.99 \pm 0.01$	$75 \pm 1$	$0.98 \pm 0.02$
	MP2 (Ref. 3)	2.93	39.5	1.29

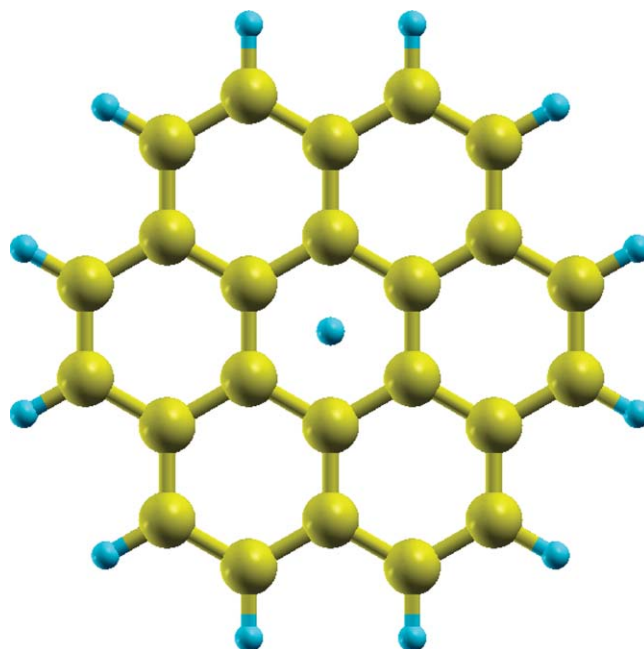


FIG. 3. Top view geometry of the H–coronene system. Carbon atoms are in yellow, hydrogens in blue.

also the same as those used in the DMC calculations, as in the hydrogen–benzene calculations.

For the DMC calculations, we used 384 000 walkers distributed on 4800 cores, and simulation lengths between 12 000 and 20 000 steps, resulting in statistical errors on each energy point between 2 and 3 meV (one standard deviation). For all points on the binding energy curve we used the Jastrow factor optimized for the system with the hydrogen at a distance of 3.0 Å from the plane of the molecule. The results are shown in Fig. 4, together with a fit to a Morse potential. In the figure we also show the Morse potentials fitted to the MP2 calculations for the same hollow geometry. Binding energy curves for a bridge and a top site were also calculated,<sup>3</sup>

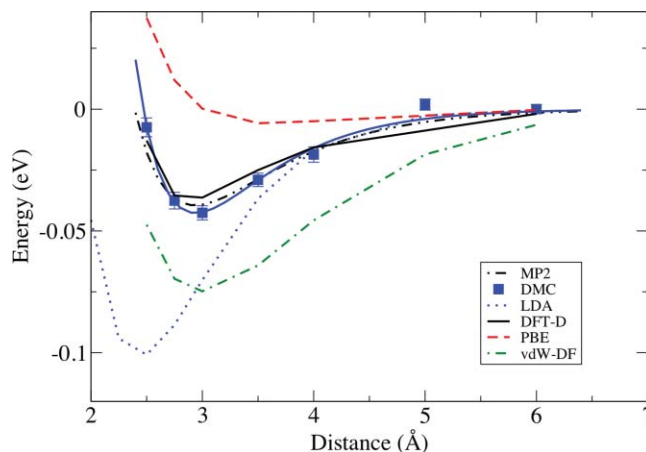


FIG. 4. Binding energy curve for H on coronene. Blue squares: DMC calculations; solid blue line: Morse potential fitted to the DMC data; double dotted-dashed line: MP2 data (Ref. 3); black line: DFT-D; red dashed line: PBE; green chain line: vdW-DF; blue dotted line: LDA.

and they are all very similar, with the hollow geometry having a slightly larger binding energy.

The DMC value for the hydrogen–coronene binding energy is  $43 \pm 3$  meV, which compares well with the MP2 value 39.5 meV.<sup>3</sup> The DMC equilibrium distance is  $x_0 = 2.93 \pm 0.04$  Å, which also agrees very well with the MP2 result. The results are summarized in Table I.

With DFT we find that DFT-D<sup>40</sup> agrees well with DMC and MP2 calculations as in the hydrogen–benzene system. Not surprisingly, LDA overestimates the binding energy, while PBE underestimates it, and vdW-DF also overestimates it by around 30 meV.

### C. Hydrogen on graphene

The graphene layer was represented with a  $5 \times 5$  surface unit cell, containing 50 carbon atoms, with a carbon–carbon distance of 1.423 Å. In the DFT calculations, we put the hydrogen atom at the origin (see Fig. 5). During geometry optimization, we fixed the hydrogen and a carbon atom at the center of the cell; the carbon atom was fixed so as to prevent the entire graphene sheet from translating during the structure optimization. The hydrogen–graphene distance reported here is the height difference between hydrogen and this carbon atom. Diffusion Monte Carlo energies have been calculated by placing the hydrogen atom at ten separate distances from the graphene layer, between 1.68 and 7.4 Å. Since the exact position of the hydrogen atom only makes a small difference in the binding energy in coronene, we decided to place the hydrogen atom on top of a carbon atom (see Fig. 5), as this is where the H eventually ends up in the chemisorbed state.

As with the coronene case, the DMC calculations were performed using between 384 000 and 768 000 walkers distributed between 4800 and 19 200 cores. The Jastrow factor was optimized by minimizing the energy of the system with hydrogen at a distance of 3.16 Å from the graphene layer. Results of the calculations are shown in Fig. 6, where it is clear that the binding energy—if there is any binding—is not larger than  $\sim 10$  meV.

With DFT we find again a wide range of results. The LDA, DFT-D, PBE, and vdW-DF functionals give physisorption energy of 97, 32, 5, and 81 meV, respectively.

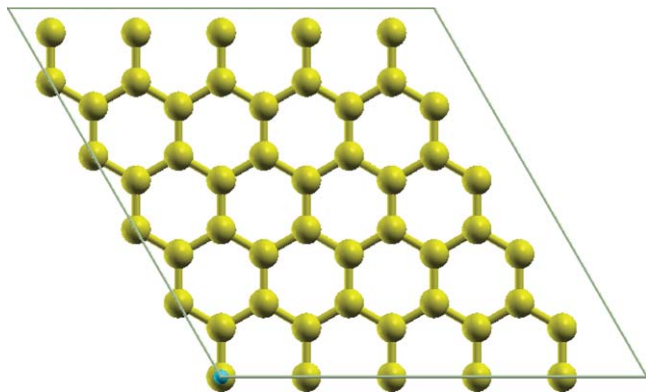


FIG. 5. Top view geometry of the primitive cell of the H–graphene system. Carbon atoms are in yellow, hydrogen in blue.

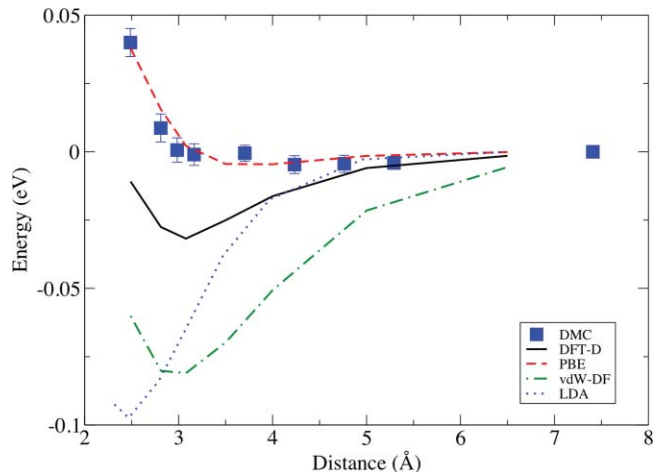


FIG. 6. Binding energy curve for H on graphene. Blue squares: DMC calculations; black line: DFT-D; red dashed line: PBE; green chain line: vdW-DF; blue dotted line: LDA.

### IV. DISCUSSION AND CONCLUSIONS

We have performed calculations of binding energy curves between a single hydrogen atom and graphene, and also between hydrogen and coronene, and hydrogen and benzene. We found that, in agreement with MP2 and CCSD(T) results, hydrogen has a small physisorption energy on benzene. A similar comparison on coronene also shows good agreement between DMC and MP2. Explicit DMC calculations on a fully periodic layer of graphene show that this physisorption minimum only has a depth of  $5 \pm 5$  meV. We note that DFT with various exchange–correlation functionals gives a wide range of results on all three systems. On graphene, the LDA, PBE, DFT-D, and vdW-DF functionals give physisorption energies of 97, 5, 32, and 81 meV, respectively.

The present results seem to indicate that extrapolation of results obtained on acenes of increasingly larger size will not necessarily produce results indicative of the behavior of a fully formed graphene layer. This is particularly true if the quantum chemistry method of choice is MP2, which cannot be used on zero gap systems.

However, we make this statement with all due caution. Despite the good agreement between DMC and MP2 calculations on coronene, and between DMC and MP2 and CCSD(T) on benzene, we must point out that the present DMC calculations are still affected by systematic errors, coming from the fixed-node approximation, and the locality or the T-move approximations in conjunction with the use of nonlocal pseudopotentials. On the energy scales involved, the size of these errors is not small, and the main reason why DMC and MP2 agree so well on coronene is mainly because of large cancellation of errors. It is probably reasonable to assume that the same scenario also applies to calculations on graphene, where only DMC calculations are available. A second possible source of error in the periodic calculations comes from  $\mathbf{k}$ -point sampling and DMC finite size errors. Although we use quite a large unit cell, sampling is limited to the gamma point. Improved  $\mathbf{k}$ -point sampling may also alter the results.

The present work is part of a wider effort aimed at investigating systems in which weak van der Waals interactions are

crucial to the binding. These systems present significant challenges to DFT methods, and we have shown that even recent state-of-the-art van der Waals corrected DFT methods may not be accurate enough. Traditional quantum chemistry methods can describe van der Waals interactions very precisely, but they cannot yet routinely handle extended systems with more than a few atoms per unit cell. The present work presents further evidence that DMC methods may have a very important role to play for these systems.

## ACKNOWLEDGMENTS

This research used resources of the Oak Ridge Leadership Computing Facility, located in the National Center for Computational Sciences at Oak Ridge National Laboratory, which is supported by the Office of Science of the Department of Energy under Contract No. DE-AC05-00OR22725. We are also grateful to UCL research computing for allocation of resources on Legion. The work of D.A. and A.M. was conducted as part of a EURYI scheme award as provided by EPSRC (see [www.esf.org/euryi](http://www.esf.org/euryi)). The work of A.M. is also supported by the European Research Council.

- <sup>1</sup>M. Hirama, T. Ishida, and J. Aihara, *J. Comput. Chem.* **24**, 1378 (2003).
- <sup>2</sup>V. Le Page, T. P. Snow, and V. M. Bierbaum, *Astrophys. J.* **704**, 274 (2009).
- <sup>3</sup>M. Bofanti, R. Martinazzo, G. Tantardini, and A. Ponti, *J. Phys. Chem. C* **111**, 5825 (2007).
- <sup>4</sup>M. Hentesche, H. Hermann, D. Lindackers, and G. Selfert, *Int. J. Hydrogen Energy* **32**, 1530 (2007).
- <sup>5</sup>X. Zhao, R. A. Outlaw, J. J. Wang, M. Y. Zhu, G. D. Smith, and B. C. Holloway, *J. Chem Phys.* **124**, 194704 (2006).
- <sup>6</sup>T. Zecho, A. Güttler, X. Sha, B. Jackson, and J. Küppers, *J. Chem. Phys.* **117**, 8486 (2002).
- <sup>7</sup>X. Sha, B. Jackson, and D. Lemoine, *J. Chem. Phys.* **116**, 7158 (2002).
- <sup>8</sup>E. Ghio, L. Matera, C. Salvo, F. Tommasini, and U. Valbusa, *J. Chem. Phys.* **73**, 557 (1980).
- <sup>9</sup>M. Dion, H. Rydberg, E. Schroder, D. C. Langreth, and B. I. Lundqvist, *Phys. Rev. Lett.* **92**, 246401 (2004).
- <sup>10</sup>A. Tkatchenko and M. Scheffler, *Phys. Rev. Lett.* **102**, 073005 (2009).
- <sup>11</sup>J. Klimeš, D. R. Bowler, and A. Michaelides, *J. Phys. Condens. Matter* **22**, 022201 (2010).
- <sup>12</sup>W. M. C. Foulkes, L. Mitáš, R. J. Needs, and G. Rajagopal, *Rev. Mod. Phys.* **73**, 33 (2001).
- <sup>13</sup>I. G. Gurtubay and R. J. Needs, *J. Chem. Phys.* **127**, 124306 (2007).
- <sup>14</sup>N. D. Drummond and R. J. Needs, *Phys. Rev. Lett.* **99**, 166401 (2007).
- <sup>15</sup>J. Ma, D. Alfè, A. Michaelides, and E. Wang, *J. Chem Phys.* **130**, 154303 (2009).
- <sup>16</sup>J. Ma, D. Alfè, A. Michaelides, and E. Wang, *Phys. Rev. Lett.* (submitted).
- <sup>17</sup>M. Pozzo and D. Alfè, *Phys. Rev. B* **77**, 104103 (2008).
- <sup>18</sup>E. Sola, J. P. Brhodholt, and D. Alfè, *Phys. Rev. B* **79**, 024107 (2009).
- <sup>19</sup>E. Sola and D. Alfè, *Phys. Rev. Lett.* **103**, 078501 (2009).
- <sup>20</sup>C. Filippi, S. B. Healy, P. Kratzer, P. Pehlke, and M. Sheffler, *Phys. Rev. Lett.* **89**, 166102 (2002).
- <sup>21</sup>M. Pozzo and D. Alfè, *Phys. Rev. B* **78**, 245313 (2008).
- <sup>22</sup>C. J. Umrigar, J. Toulouse, C. Filippi, S. Sorella, and R. G. Hennig, *Phys. Rev. Lett.* **98**, 110201 (2007).
- <sup>23</sup>J. Toulouse and C. J. Umrigar, *J. Chem. Phys.* **126**, 084102 (2007).
- <sup>24</sup>L. Mitáš, E. L. Shirley, and D. M. Ceperley, *J. Chem. Phys.* **95**, 3467 (1991).
- <sup>25</sup>M. Casula, *Phys. Rev. B* **74**, 161102 (2006).
- <sup>26</sup>J. R. Trail and R. J. Needs, *J. Chem. Phys.* **122**, 014112 (2005); **122**, 174109 (2005).
- <sup>27</sup>S. Baroni, A. Dal Corso, S. de Gironcoli, and P. Giannozzi. Available online at: <http://www.pwscf.org>.
- <sup>28</sup>D. Alfè and M. J. Gillan, *Phys. Rev. B*, **70**, 161101(R) (2004).
- <sup>29</sup>CPMD, <http://www.cpmd.org/>. Copyright IBM Corp. 1990–2008, copyright MPI für Festkörperforschung Stuttgart 1997–2001.
- <sup>30</sup>G. Kresse and J. Furthmüller, *Comput. Mater. Sci.* **6**, 15 (1996).
- <sup>31</sup>N. Troullier and J. L. Martins, *Phys. Rev. B* **43**, 1993 (1991).
- <sup>32</sup>P. Blöchl, *Phys. Rev. B* **50**, 17953 (1994).
- <sup>33</sup>G. Kresse and D. Joubert, *Phys. Rev. B* **59**, 1758 (1999).
- <sup>34</sup>J. P. Perdew, K. Burke, and M. Ernzerhof, *Phys. Rev. Lett.* **77**, 3865 (1996).
- <sup>35</sup>M. Elstner, P. Hobza, T. Frauenheim, S. Suhai, and E. Kaxiras, *J. Chem. Phys.* **114**, 5149 (2001).
- <sup>36</sup>A. Gavezzotti, *J. Am. Chem. Soc.* **105**, 5220 (1983); J. D. Dunitz and A. Gavezzotti, *Acc. Chem. Res.* **32**, 677 (1999); G. Filippini and A. Gavezzotti, *Acta Crystallogr., Sect. B: Struct. Sci.* **49**, 868 (1993).
- <sup>37</sup>J. Klimeš, D. R. Bowler, and A. Michaelides, *Phys. Rev. B* (submitted); arXiv:1102.1358v1.
- <sup>38</sup>G. Roman-Perez and J. M. Soler, *Phys. Rev. Lett.* **103**, 096102 (2009).
- <sup>39</sup>R. J. Needs, M. D. Towler, N. D. Drummond, and P. López Ríos, *J. Phys.: Condensed Matter* **22**, 023201 (2010).
- <sup>40</sup>A DFT-D value of 38.1 meV was also recently reported by R. M. Ferullo, M. F. Domanchic, and N. J. Castellani, *Chem. Phys. Lett.* **500**, 283 (2010).
- <sup>41</sup>A. Kokalj, *Comput. Mater. Sci.* **28**, 155 (2003); code available from <http://www.xcrysden.org/>.